Studies of Zone Melting. V. The Solid-Liquid Equilibrium and Zone Melting of the Bibenzyl-Diphenylacetylene System

Hidemoto NOJIMA* and Seigou AKEHI

Department of Industrial Chemistry, Faculty of Engineering, Meiji University, Ikuta, Tama-ku, Kawasaki 214

(Received January 17, 1979)

The phase diagram of the bibenzyl–diphenylacetylene system was determined in detail from DSC by using the following equation:

$$T = \alpha\sqrt{F'} + \beta,$$

where T is the temperature; F', the corrected fraction melted, calculated by the use of the area for the vertex of the peak instead of the total peak area and α and β, the constants. Then, the melting and freezing temperatures were obtained from a plot of T *vs.* $\sqrt{F'}$ by the use of the values of β and $\alpha+\beta$ respectively. The results show the formation of solid solutions with a minimum melting point, at which difficulty in determining the composition often arises from the fact that the slopes of both the solidus and liquidus curves are zero. This could be overcome by multipass zone melting for two samples containing 20 and 30 wt % of diphenylacetylene; after 45 zone passes, the composition of the minimum melting point was found to be 26.4% at the end. Also, by Herington's theory, it has been revealed that zone-melting experiments were attained almost at equilibrium.

The behavior of a solute during the zone melting of binary mixtures can be interpreted to some extent by the phase diagrams of these mixtures. Conversely, it follows that a type of phase diagram may be shown from the results of zone-melting experiments. Herington[1] has theoretically described the relation between the zone-melting behavior and the phase diagrams of binary mixtures. However, few applications of zone melting to the study of the phase diagrams of organic compounds have been reported. By the combined use of zone melting and the differential thermal analysis, Jonchich *et al.*[2] have reconstructed the phase diagram of the phenanthrene–anthracene system, which had previously been reported by Bradley and Marsh,[3] and Kofler.[4]

It has also been reported[5] that the bibenzyl–diphenylacetylene system forms a continuous series of solid solutions with Roozeboom's Type I:[6] the freezing points of all mixtures lie between those of the pure components. The present authors, however, have argued against the above conclusion on the basis of the difference between the crystal structures and the molecular sizes of these two compounds.[7] The present work has been carried out in order to prove our argument against the formation of the phase diagram of Roozeboom's Type I; the solid-liquid equilibrium for this system is investigated in detail by means of both zone melting and DSC (differential scanning calorimetry) in the search for a useful equation for determining the melting and freezing temperatures from the relation between the temperature and the corrected fraction melted in DSC. It has thus been verified that this system does not form a continuous series of solid solutions, as has reported previously,[5] but forms solid solutions with a minimum melting point: Roozeboom's Type III.[6] In this case, the solidus and liquidus curves meet at a minimum temperature, at which the phases existing in equilibrium have the same composition. The slopes of both the solidus and liquidus curves at the minimum melting point are zero, in accordance with the Gibbs-Konovalow rule, and the difference between the melting and freezing temperatures on both sides in the vicinity of the minimum melting point is usually slight. Hence, it is often difficult for the composition at the minimum melting point to be determined precisely by ordinary thermal analysis. In this work, the composition of the minimum melting point was determined precisely by multipass zone-melting experiments for two specimens with initial concentrations at both sides near the composition of the minimum melting ponit, which has roughly been predetermined by DSC.

Moreover, the evaluation of the deviation from equilibrium in the multipass zone-melting experiments is discussed by means of Herington's theory.

No zone-melting experiments have previously been reported for this system.

Theoretical

Determination of the Solidus and Liquidus Curves by DSC. A typical DSC peak for a binary mixture forming a solid solution is shown in Fig. 1, in which the fraction melted, F, at a definite temperature, *e.g.*, T_n, is given in the following way:[11,13]

$$F = \frac{\text{area ACHA}}{\text{area AEFA}}. \tag{1}$$

Strictly speaking, Eq. 1 is valid only when the heats of fusion of the constituents are nearly equal and when the heat of mixing can be neglected in comparison with them. From Fig. 1, Eq. 1 may be rewritten as follows:

$$F = \frac{\text{area BCHB}+\text{area ABJA}}{\text{area BDGB}+\text{area DEFD}+\Delta a}, \tag{2}$$

where Δa denotes the difference between the area ABJA and the area FGIF. Equation 2 may further be rewritten as follows:

$$F = \frac{\text{area BCHB}+\text{area ABJA}}{\text{area BDGB}} \cdot \frac{\text{area BDGB}}{\text{area BDGB}+\text{area DEFD}+\Delta a}. \tag{3}$$

Assuming that the area ABJA is small and can be

neglected in comparison with the area BCHB, the following equation is obtained:

$$F = \frac{\text{area BCHB}}{\text{area BDGB}} \cdot \frac{\text{area BDGB}}{\text{area BDGB}+\text{area DEFD}+\Delta a}. \quad (4)$$

In Eq. 4 it is convenient to put as

$$F' = \frac{\text{area BCHB}}{\text{area BDGB}}, \quad (5)$$

$$K = \frac{\text{area BDGB}}{\text{area BDGB}+\text{area DEFD}+\Delta a}. \quad (6)$$

Hence, the following equation is obtained:

$$F = F'K \quad (7)$$

where F' is the fraction melted as calculated by the use of the areas of the ΔBDG and ΔBCH triangles instead of by the calculation of the total peak area and the area ACHA, as represented by Eq. 1, and where K is the constant, depending upon the samples. It follows that the relation between F and F' is represented by Eq. 7. We will term F' the corrected fraction melted. As will be described below the experimental results are better interpreted experientially by F' than by F.

Furthermore, the conclusion presented below may be made for the corrected fraction melted, F'. From Fig. 1, the following equations are obtained:

$$\text{area ADFA} = \text{area BDFB} + \text{area ABJA}, \quad (8)$$

$$\text{area BDGB} = \text{area BDFB} + \text{area IFGI}. \quad (9)$$

From Eqs. 8 and 9, the following equation is then obtained:

$$\text{area ADFA} = \text{area BDGB} + \text{area ABJA} - \text{area IFGI}. \quad (10)$$

Putting the second and third terms on the right-hand side of Eq. 10 as

$$\Delta b = \text{area ABJA} - \text{area IFGI}, \quad (11)$$

Eq. 10 is rewritten as follows:

$$\text{area ADFA} = \text{area BDGB} + \Delta b. \quad (12)$$

Assuming that Δb is small and can be neglected in comparison with the area BDGB, Eq. 13 is obtained:

$$\text{area ADFA} = \text{area BDGB}. \quad (13)$$

The following relation for F' is obtained, together with the assumption described previously; *i.e.*, the area ABJA can be neglected in comparison with the area BCHB:

$$F' = \frac{\text{area BCHB}}{\text{area BDGB}} = \frac{\text{area ACHA}}{\text{area ADFA}}. \quad (14)$$

In the DSC curve, the abscissa indicates the temperature, while the ordinate indicates the millicalories per second. Moreover, in the DSC chart, the time and the temperature can be read off from the abscissa and the ordinate respectively. Therefore, the assumption presented below and Fig. 1 seems to be true. Since the temperature, T, in the DSC chart is the linear function of time, t, for the line $\overline{BH}$ in Fig. 1, the following equation is obtained:

$$T = kt + l, \quad (15)$$

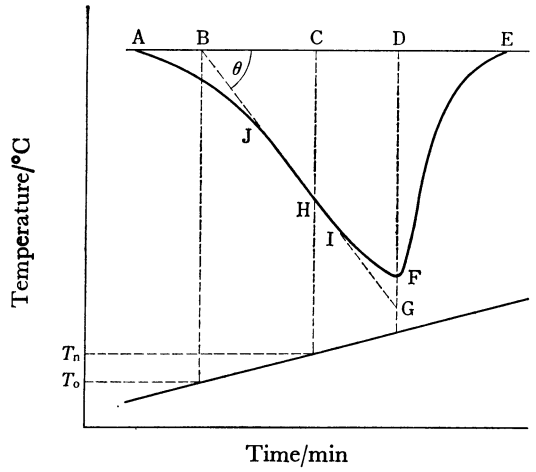

Fig. 1. Schematic diagram for the derivation of Eq. 32.

where k and l are constants. Much as in Eq. 15, for the line $\overline{BC}$ in Fig. 1, Eq. 16 is obtained:

$$T = mt + n, \quad (16)$$

where m and n are constants. Let v denote the chart speed; Eqs. 15 and 16 can then be rearranged as follows:

$$T = \frac{\overline{BH}}{v}k + l, \quad (17)$$

$$T = \frac{\overline{BC}}{v}m + n. \quad (18)$$

Rewrite Eqs. 17 and 18 as follows:

$$\overline{BH} = \frac{v}{k}T - \frac{lv}{k}, \quad (19)$$

$$\overline{BC} = \frac{v}{m}T - \frac{nv}{m}, \quad (20)$$

where it is convenient to put $(v/k)\equiv a$, $(-lv/k)\equiv b$, $(v/m)\equiv c$, and $(-nv/m)\equiv d$. Therefore, Eqs. 21 and 22 are obtained:

$$\overline{BH} = aT + b, \quad (21)$$

$$\overline{BC} = cT + d. \quad (22)$$

As is obvious from Fig. 1, when $\overline{BH}$ is zero; $\overline{BC}$ is also to be zero, and let T_0 be the temperature. Substituting the above conditions into Eqs. 21 and 22 yields Eqs. 23 and 24:

$$T_0 = -\frac{b}{a}, \quad (23)$$

$$T_0 = -\frac{d}{c}. \quad (24)$$

Therefore,

$$ad = bc. \quad (25)$$

The area, S, of the triangle ΔBCH is

$$S = \frac{1}{2} \times \overline{BC} \times \overline{CH} = \frac{1}{2}(aT+b)(cT+d)\sin\theta. \quad (26)$$

Equation 26 is rewritten by Eq. 25 as follows:

$$S = \frac{1}{2}(acT^2+2bcT+bd)\sin\theta. \quad (27)$$

Then, Eq. 28 is obtained:

$$S = \frac{1}{2}ac\left(T+\frac{b}{a}\right)^2 \sin\theta. \quad (28)$$

The area, S_0, of the triangle ΔBDG is represented by

$$S_0 = \frac{1}{2} \times \overline{BD} \times \overline{DG} = \frac{1}{2} \times \overline{BD} \times \overline{BG} \sin\theta. \quad (29)$$

From Eqs. 28 and 29, the corrected fraction melted, F', is obtained by

$$F' = \frac{S}{S_0} = \frac{ac}{\overline{BD} \times \overline{BG}}\left(T+\frac{b}{a}\right)^2, \quad (30)$$

by solving Eq. 30 for T, and from Eq. 23 the following equation is obtained:

$$T = \sqrt{\frac{\overline{BD} \times \overline{BG}}{ac}}\sqrt{F'} + T_0. \quad (31)$$

Since both $\sqrt{(\overline{BD} \times \overline{BG})/ac}$ and T_0 are constants, it is convenient to put these constants as α and β respectively. Then, we obtain Eq. 32:

$$T = \alpha\sqrt{F'} + \beta. \quad (32)$$

The DSC curve is the same in nature as the differential thermal analysis curve,[10] and the vertex of the peak (Point F in Fig. 1) most accurately reflects the melting point,[11] *i.e.*, the conclusion of the melting. Furthermore, in a binary system the melting temperature is signified by the first departure of the base line from the normal (Point A in Fig. 1), while the freezing temperature is signified by the vertex of the peak,[12] at which F'=(area ADFA/area ADFA)=1, as may be seen in Fig. 1.

From the above description, the melting temperature, corresponding to the solidus temperature, may be given by the intercept, β, of Eq. 32 when F' is zero, and the freezing temperature, corresponding to the liquidus temperature, may be obtained from the value of $\alpha+\beta$ when F' is unity, while the melting range is indicated by the slope, α.

Multipass Zone Melting. An equation for the solute distribution resulting from an infinite number of zone passes has been derived by Pfann.[8] This equation is, however, applicable only to a system with constant distribution coefficient. Pfann's equation for the ultimate distribution is as follows:

$$C(Z) = A\exp(BZ) \quad (33)$$

where $C(Z)$ is the solute concentration at the point Z from the top of the sample after the ultimate distribution has been reached and where A and B are constants obtainable from Eqs. 34 and 35:

$$k = \frac{B}{e^B-1}, \quad (34)$$

$$A = \frac{C_0BL}{e^{BL}-1}, \quad (35)$$

where C_0 is the initial concentration of the solute; L, the length of the sample, and k, the constant distribution coefficient. Rewrite Eq. 33 as follows:

$$\ln C(Z) = BZ + \ln A. \quad (36)$$

Moreover, from Eq. 36, the solute distribution at a small distance, dZ, further along the sample is give by

$$\ln C(Z+dZ) = B(Z+dZ) + \ln A. \quad (37)$$

The following equation is derived by subtracting Eq. 36 from 37:

$$\ln\frac{C(Z+dZ)}{C(Z)} = B dZ. \quad (38)$$

Equation 38 is rewritten as follows:

$$C(Z+dZ) = C(Z)\exp(BdZ). \quad (39)$$

Although Eq. 39 is applicable strictly to a system with a constant distribution coefficient, as has already been described, this equation is also approximately applicable to a system with a slight variation in the concentration near the end of the phase diagram. When the distribution coefficient, however, varies appreciably, Eq. 39 fails to be useful.

Herington[1] has extended Pfann's theory to binary systems when the distribution coefficients are dependent on the concentration.

For what follows, it is necessary to summarize his method for calculating the ultimate distribution curve, which should be calculated by the following procedures:

1. Depict a plot of the equilibrium distribution coefficient, k_i, against the concentration, C, of the solute in the solid phase with the aid of the phase diagram.

2. Obtain the values of B_i from Eq. 40 with the values of k_i from this plot. The subscript i is used to designate the concentration dependence of these values; the values of B_i can be obtained essentially from the table of the Einstein function,

$$k_i = \frac{B_i}{e^{B_i}-1}. \quad (40)$$

Plot the function B_i against C from the resulting values.

3. Choose, near one end of the phase diagram, an arbitrary value of $C(Z)$. This value must, however, be chosen in the part of the phase diagram applicable to the initial uniform composition of the charge.

4. Read the value of B_i corresponding to the solid composition $C(Z)$ from the graph obtained in Section 2; let this value be $B_i(Z)$.

5. Calculate, by means of Eq. 41, the value of $C(Z+1/d)$, applicable to the composition at a distance, $1/d$, of a zone length further along the specimen,

$$C\left(Z+\frac{1}{d}\right) = C(Z)\exp\left\{\frac{B_i(Z)}{d}\right\}. \quad (41)$$

6. Using this value for $C(Z+1/d)$, repeat the calculation discussed in Sections 4 and 5 to obtain a new value of B_i, that is, the value of $B_i(Z+1/d)$, and then calculate $C(Z+2/d)$ by means of Eq. 42:

$$C\left(Z+\frac{2}{d}\right) = C\left(Z+\frac{1}{d}\right)\exp\left\{\frac{B_i\left(Z+\frac{1}{d}\right)}{d}\right\}. \quad (42)$$

The calculations should similarly be iterated until the composition asymptotically approaches that of a pure component or the composition of the minimum melting point.

Equations 41 and 42 are rearranged in the following general form:

$$C\left(Z+\frac{n+1}{d}\right) = C\left(Z+\frac{n}{d}\right)\exp\left\{\frac{B_i}{d}\left(Z+\frac{n}{d}\right)\right\}, \quad (43)$$

n=0,1,2,3,……

Experimental

Materials. The bibenzyl and diphenylacetylene used for the determination of the phase diagram were purified by zone refining, followed by recrystallization once from ethanol.

For the multipass zone-melting experiments, a larger quantity of the bibenzyl as the solvent was used than that of the diphenylacetylene used as the solute. However, the zone-refining apparatus** which we employed for refining the chemicals cannot treat a large quantity of chemicals; hence, bibenzyl purified only by recrystallization once from ethanol was used, while the diphenylacetylene was purified by zone refining, followed by recrystallization once from ethanol.

For the determination of the phase diagram, ten specimens of the bibenzyl–diphenylacetylene mixtures (containing 5, 10, 20, 30, 40, 50, 60, 70, 80, and 90 wt % of diphenylacetylene) were prepared by melting in Pyrex ampoules under a dry nitrogen atmosphere and by grinding to powder after the ampoules had been taken out.

For multipass zone-melting experiments, two bibenzyl–diphenylacetylene mixtures containing 20 and 30 wt % of diphenylacetylene were prepared by melting in Pyrex ampoules under a dry nitrogen atmosphere and by grinding to powder after the ampoules had been taken out.

These mixtures were charged in a length of 30 cm in Pyrex tubes with an inner diameter of 0.7 cm and outer diameter of 0.9 cm. Then the tubes were sealed off under a dry nitrogen atmosphere of about 0.9 atm.

Apparatus and Procedures. The melting and freezing temperatures were determied with a Shimadzu differential scanning calorimeter, SC-20, under the following conditions: heating rate, 1 °C/min; chart speed, 40 mm/min; range, ±5 mcal/s.

The multipass zone-melting experiments were carried out with the apparatus described in a previous paper[9] and under the following conditions: zone travel rate, 0.73 cm/h; zone length, 3 cm; zone temperature, 61±1 °C; the number of zone passages, 45.

The samples after zone melting were cut into 3-cm-long divisions. The concentration of diphenylacetylene in each division was determined spectrophotometrically in an ethanol solution by the use of a Hitachi 101 spectrophotometer at a wavelength of 305 nm.

Results and Discussion

The Phase Diagram of the Bibenzyl–Diphenylacetylene System. With the results of DSC, the temperature, T, was plotted against the square root of the corrected fraction melted, $\sqrt{F'}$, as is shown in Fig. 2. From the resulting straight lines, the melting and freezing temperatures were calculated by means of Eq. 32.

As may be seen in Fig. 2, for pure components, that is, bibenzyl or diphenylacetylene, it is in conflict with the phase rule that the relation between T and $\sqrt{F'}$ obeys Eq. 32, like a mixture. Such behavior observed in pure components is probably due to the impossibility of obtaining an absolutely pure substance and a time lag caused mainly by the finite thermal conductivity in the samples during fusion.

Therefore, the value of α in Eq. 32 for a pure component, which may correspond to the apparent melting range caused by the above reasons, should be added to all the observed melting temperatures of the bibenzyl–diphenylacetylene mixtures for the corrections of the temperatures. These corrections were made by using the value, 1 °C, of pure bibenzyl for the specimens with 5 to 20% of diphenylacetylene, and by using the value, 0.8 °C, of pure diphenylacetylene for the specimens with 30 to 90% of diphenylacetylene. The results obtained are presented in Table 1 and Fig. 3; the old data reported by Pascal *et al.*[5] are also shown, represented by the broken lines in Fig. 3.

Indeed, such systems as the azobenzene–stilbene and diphenylacetylene–stilbene form a continuous series of solid solutions because of the close resemblances

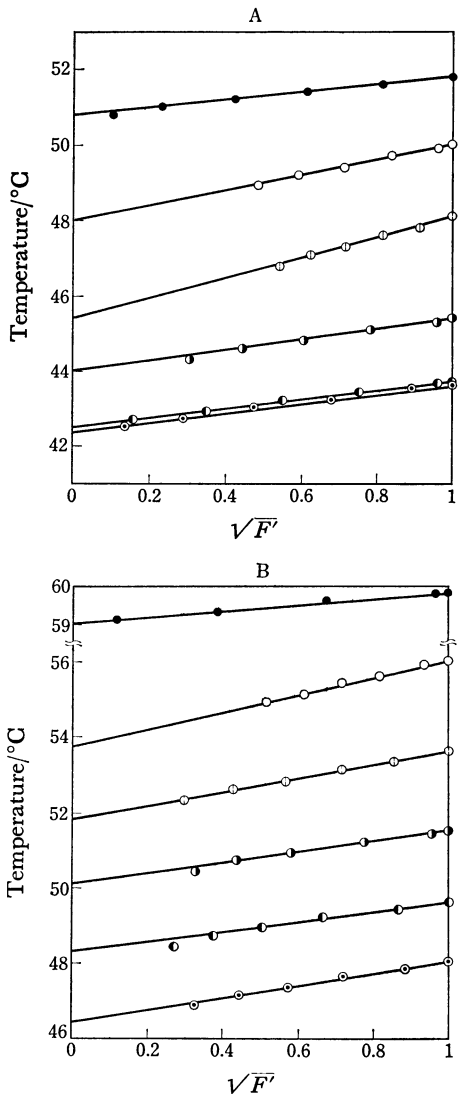

Fig. 2. Relation between the temperature and square root of the corrected fraction melted.
A: ●; 100% of bibenzyl, ○; 5% of diphenylacetylene, ◑; 10% of diphenylacetylene, ◐; 20% of diphenylacetylene, ⊙; 30% of diphenylacetylene, ◑; 40% of diphenylacetylene. B: ●; 100% of diphenylacetylene, ○; 90% of diphenylacetylene, ◑; 80% of diphenylacetylene, ◑; 70% of diphenylacetylene, ◐; 60% of diphenylacetylene, ⊙; 50% of diphenylacetylene.

** Shimadzu cryogenic zone-refiner, CZ-1.

Table 1. The melting and freezing temperatures for the bibenzyl-diphenylacetylene system

Concentration of diphenylacetylene wt%	Melting temp °C	Freezing temp °C
0	51.8	51.8
5	49.0	50.0
10	46.4	48.1
20	43.5	43.7
30	43.2	43.6
40	44.8	45.4
50	47.2	48.0
60	49.1	49.6
70	50.9	51.5
80	52.6	53.6
90	54.5	56.0
100	59.8	59.8

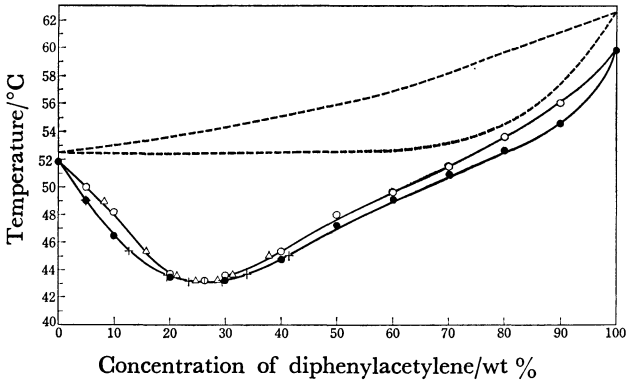

Fig. 3. Phase diagram of the bibenzyl-diphenylacetylene system.
○: Freezing temperature determined by DSC, ●: meting temperature determined by DSC, △: composition of liquid phase calculated by the Herington's theory, +: composition of solid phase calculated by the Herington's theory, ⓘ: composition of minimum melting point determined by multipass zone-melting experiments, ----: solidus and liquidus curves reported by Pascal *et al.*[5]

of the crystal structures and molecular sizes among these compounds,[7] but bibenzyl is somewhat different in these factors[7] from the above three compounds.

In consequence of these differences in the crystal structure and molecular size, the bibenzyl–diphenylacetylene system may deviate from an ideal solution and may form solid solutions with a minimum melting point, as has previously been predicted.

The Determination of the Composition of the Minimum Melting Point by Multipass Zone-melting Experiments. Figure 4 and Table 2 show the relation between the concentration of diphenylacetylene and the distance in zone lengths along the specimens after 45 zone passes for two specimens containing initially 20 and 30 wt % of diphenylacetylene respectively.

As is obvious from Fig. 3, the distribution coefficient of diphenylacetylene in bibenzyl for 20% of diphenylacetylene is less than unity, whereas, in the case of 30% of diphenylacetylene, the distribution coefficient

Table 2. Distribution of diphenylacetylene in bibenzyl after 45 zone passes

Distance in zone length $\left(\frac{x}{l}\equiv Z\right)$	Concentration of diphenylacetylene (wt %); initial concentration 20 wt % of diphenylacetylene	Concentration of diphenylacetylene (wt %); initial concentration, 30 wt % of diphenylacetylene
0.5	1.1	56.8
1.5	3.7	42.6
2.5	14.1	34.5
3.5	17.0	29.4
4.5	25.0	28.0
5.5	26.1	27.0
6.5	25.2	27.2
7.5	25.7	27.3
8.5	26.4	26.4
9.5	26.3	26.4
10.5	25.6	27.8

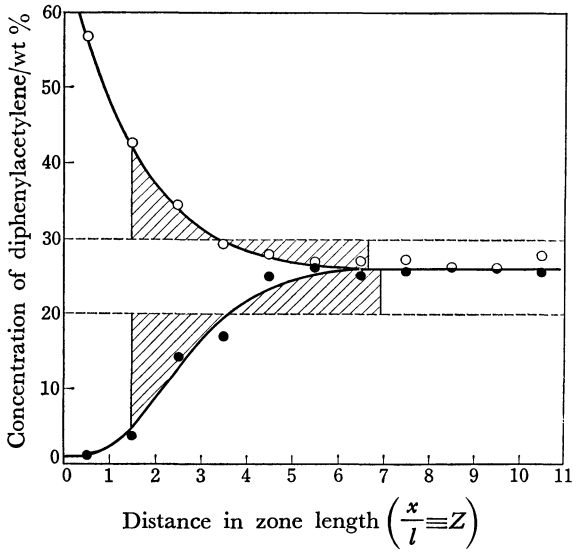

Fig. 4. Distrbution of diphenylacetylene in two samples after 45 zone passes.
●: Initial concentration: 20% of diphenylacetylene,
○: initial concentration: 30% of diphenylacetylene,
▨: the areas for calculating material balance after 45 zone passes.

is greater than unity. Such a difference in the distribution coefficients is reflected in the two distribution curves of diphenylacetylene shown in Fig. 4.

The two curves are each observed to approach a constant value gradually; this value may correspond to the composition of the minimum melting point. This phenomenon is analogous to that occurring with the fractional distillation of the azeotropic mixtures with a minimum boiling point.

A mixture with the composition of the minimum melting point must be, in principle, obtained at the end of the specimen. However, other impurities tend to concentrate at the end of the specimen; hence, the values at eight fractions from the top of the samples are adopted as the composition of the minimum melting point in both samples. Thus, we obtained the value

of 26.4% at the temperature of 43.2 °C.

The Evaluation of the Extent of Deviation from Equilibrium in the Multipass Zone Melting. Although the composition at the near end of the specimen gradually approaches the composition of the minimum melting point as a result of repeated zone passes, the compositions at the upper regions of the specimens (left part in Fig. 4) seem to become not necessarily equal to the compositions estimated from the phase diagram, depending upon the extent of devaition from equilibrium, which mainly varies with the zone-travel rate.

As is well known, the solute distribution between the solid and liquid phases in a non-equilibrium state is indicated by the effective distribution coefficient. Hence, the extent of the deviation from equilibrium in multipass zone-melting experiments will be discussed by estimating the effective distribution coefficients by means of Herington's method, which will, in the present case, be employed in the reverse of its original purpose so as to calculate the distribution coefficients from the observed distribution curve.

The boundary condition in Eq. 43 must be determined from the viewpoint of the material balance. The values of the Z and $n+1$ in Eq. 43 should be chosen so as to equalize the shaded areas divided into two portions across the lines indicating the initial concentrations for the two curves in Fig. 4. In the present case, the value of d is determined for convenience as unity, for the samples were cut into fractions equal to one zone length. Then, Eq. 43 is rewritten as follows:

$$C\{Z+(n+1)\} = C(Z+n)\exp\{B_1(Z+n)\}. \quad (44)$$

It is obvious from Fig. 4 that the numerical value of Z was defined as 1.5 for both curves. Therefore, $(n+1)$ equals 6 for both the lower and upper curves in Fig. 4. By substituting successively into Eq. 44 the values obtained from the curves in Fig. 4, the respective value of B_i is calculated. The effective distribution coefficient is calculated by substituting the value obtained above into B_i in Eq. 40; of course, the k_i in Eq. 40 should be replaced by the k_e, symbolizing the effective distribution coefficient.

From the resulting effective distribution coefficient, the solute concentration in the liquid phase, C_l, is obtained by the definition of the distribution coefficient, *i.e.*, $k_e=C_s/C_l$, in which C_s is identical with $C(Z+n)$ in Eq. 44.

The results thus obtained are presented in Table 3. The relation between the solid and liquid phases is also shown, together with the results from DSC in Fig. 3, so as to indicate clearly the deviation from equilibrium.

It is revealed that the magnitude of deviation from equilibrium is fairly slight. This is, of course, a fact that does not commonly appear, but it is valid for this experiment. As one reason for such a slight departure from equilibrium, it may be considered that the difference between the melting and freezing temperatures is quite small in this system, as is shown in Fig. 3. Indeed, in the naphthalene–2-naphthol system, the difference between the melting and freezing temperatures is larger than that in the bibenzyl–diphenylacetylene system. Hence, it is shown by Herington's theory that the deviation from equilibrium is fairly great†, in contrast to the result in this work.

Table 3. The effective distribution coefficient and composition of diphenylacetylene in the liquid phase, as obtained by Herington's theory

Distance in zone length $\left(\frac{x}{l}\equiv Z\right)$	Composition of the solid phase (wt %)	Effective distribution coefficient	Composition of the liquid phase (wt %)
Initial concentration, 20 wt % of diphenylacetylene			
1.5	5	0.61	8.2
2.5	12.7	0.81	15.7
3.5	19.5	0.91	21.4
4.5	23.5	0.96	24.5
5.5	25.4	0.99	25.7
Initial concentration, 30 wt % of diphenylacetylene			
Distance in zone length $\left(\frac{x}{l}\equiv Z\right)$	Composition of the solid phase (wt %)	Effective distribution coefficient	Composition of the liquid phase (wt %)
1.5	41.4	1.10	37.6
2.5	33.8	1.07	31.5
3.5	29.7	1.04	28.5
4.5	27.4	1.04	26.3
5.5	26.4	1.01	26.1

Although, in the calculation of the corrected fraction melted, the theoretical ground is still obscure for replacing the total peak area by the area for the vertex of the peak, Eq. 20 has proved of great value as a means of determining precisely the melting and freezing temperatures in DSC, especially in the case of a peak too broad or even a noisy one.

The determination of the composition of the minimum melting point through the multipass zone-melting experiments would be applicable not only to organic systems, but also to inorganic and metallic systems, though an analytical technique must be utilized for determining the components precisely.

Conclusion

The behavior of diphenylacetylene in bibenzyl during zone melting can be well related to the phase diagram with the aid of Herington's theory. This, in other words, suggests the validity of the obtained phase diagram.

The authors wish to thank Professor Masaru Inagaki, of Meiji University, and Professor Sohachiro Hayakawa, of the Tokyo Institute of Technology, for their valuable advice.

References

1) E. F. G. Herington, "Zone Melting of Organic Compounds," Blackwell Scientific Publications, Oxford (1963),

† Evaluated by the use of the data in a previous paper.[9]

pp. 100—125.
2) M. J. Joncich and D. R. Bailey, *Anal. Chem.*, **32**, 1578 (1960).
3) G. Bradley and J. K. Marsh, *J. Chem. Soc.*, **1933**, 650.
4) A. Kofler, *Monatsh. Chem.*, **86**, 301 (1955).
5) "International Critical Tables," McGraw-Hill Book Co., New York (1928), Vol. 4, p. 163.
6) H. Schildknecht, "Zone Melting," Academic Press, New York (1966), pp. 4—12.
7) A. I. Kitaigorodskii, "Organic Chemical Crystallography," Consultants Bureau Enterprises, New York (1961), pp. 231—240.
8) W. G. Pfann, "Zone Melting," John Wiley & Sons, New York (1959), pp. 40—45.
9) H. Nojima, *Nippon Kagaku Zasshi*, **91**, 810 (1970).
10) T. Ozawa, *Netsusokutei*, **4**, 45 (1977).
11) E. M. Barrall, II, and J. F. Johonson, "Purification of Inorganic and Organic Materials," ed by M. Zief, Marcel Dekker, New York (1969), pp. 77—100.
12) Y. Otsubo, *Netsusokutei*, **1**, 107 (1974).
13) C. Plato and A. R. Glasgow, Jr., *Anal. Chem.*, **41**, 330 (1969).